ELSEVIER

Biochemical Pharmacology 63 (2002) 471–483

Biochemical Pharmacology

Modulation of apoptosis by mitochondrial uncouplers: apoptosis-delaying features despite intrinsic cytotoxicity

Oliver J. Stoetzer[a,1], Alexei Pogrebniak[a,1], Renate Pelka-Fleischer[a]
Max Hasmann[b], Wolfgang Hiddemann[a], Volkmar Nuessler[a,*]

[a]*Medizinische Klinik III, Department of Haematology and Oncology, Klinikum Grosshadern, Marchioninistr. 15, 81377 Munich, Germany*
[b]*Klinge Pharma GmbH, Department of Pharmacology, 81673 Munich, Germany*

Received 17 May 2001; accepted 15 October 2001

Abstract

Disruption of mitochondrial electron transport and opening of the so-called mitochondrial permeability transition pores (PTPs) are early events in apoptotic cell death and may be caused by the uncoupler of mitochondrial oxidation and phosphorylation, carbonyl cyanide *p*-trifluoromethoxyphenylhydrazone (FCCP). We investigated the cellular toxicity of FCCP in HL60 and CCRF-CEM cells alone or in combination with the known apoptosis inducers such as inhibitor of serine/threonine protein kinases staurosporine (Sts) and protein kinase C inhibitor chelerythrine. FCCP induced apoptotic cell death in both cell lines in a dose-dependent manner, and we were able to demonstrate an appearance of caspase-3-dependent PARP cleavage fragments with Western blot and the appearance of large (15–50 kb) DNA fragments using pulsed-field gel electrophoresis. After 2 hr of incubation with Che or Sts more than half of the cells had died by apoptosis. We observed a statistically significant delay in Sts- and Che-induced apoptotic cell death in CCRF-CEM cells when the cells were preincubated with FCCP but not with zVAD-FMK: about 50% more cells survived after pre-treatment with FCCP, as compared to 1 hr treatment with Che alone ($P < 0.05$), and 25% more cells were alive after 6 hr of treatment, as compared to 6 hr exposure to Sts alone ($P < 0.05$). The protective effect of FCCP was, however, transient and lasted only 6 hr. Treatment with aurintricarboxylic acid completely prevented Che- and Sts-induced apoptotic cell death in CCRF-CEM and HL60 cells. Incubation with Che resulted in a drop in the intracellular ATP content, predominantly distinctive in HL60, and in NAD^+ content in CCRF-CEM cells. Both ATP and NAD^+ drop were prevented with ATA, but not with FCCP or zVAD. Our data suggest that treatment with uncouplers of oxidative phosphorylation can induce apoptotic cell death in haematopoietic cell lines. However, when used in combination with serine/threonine protein kinase inhibitors FCCP can even prevent apoptosis.

Keywords: Apoptosis; FCCP; Chelerythrine; Aurintricarboxylic acid; NAD^+; Mitochondrial uncouplers

1. Introduction

It is widely accepted that disruption of mitochondrial function together with activation of caspases and fragmentation of DNA are major biochemical events in the process of programmed cell death (PCD). The events that contribute to apoptosis such as alterations in mitochondrial membrane potential [1,2], generation of reactive oxygen species [3–5], and release of caspase-activating proteins [6,7] are closely associated with mitochondrial function.

Bcl-2, a 26 kDa protein, is predominantly localized in mitochondria and is a strong inhibitor of PCD [8–10]. The exact biochemical mechanism of Bcl-2 remains unclear. Its ability to form membrane pores seems to be important for its antiapoptotic function [11,29,32]. There is preliminary evidence that Bcl-2 may communicate functionally or physically with mitochondrial proteins that govern ion transport [12].

The alterations in mitochondrial membrane potential in the time course of apoptosis are thought to occur when the large non-selective channel in the inner mitochondrial

* Corresponding author. Tel.: +49-89-7095-3137; fax: +49-89-7095-6137.
E-mail address: nuessler@gmx.net (V. Nuessler).

[1] Authors contributed equally to this work.

Abbreviations: ADH, alcohol dehydrogenase; AFC, 7-amino-4-trifluoromethylcoumarin; AIF, apoptosis-inducing factor; ATA, aurintricarboxylic acid; CCCP, carbonyl cyanide *m*-chlorophenylhydrazone; Che, chelerythrine; PTP, permeability transition pores; FCCP, carbonyl cyanide *p*-trifluormethoxyphenylhydrazone; FCS, fetal calf serum; IM, inner mitochondrial membrane; PARP, poly-(ADP-ribose) polymerase; PCD, programmed cell death; PFGE, pulsed-field gel electrophoresis; Sts, staurosporine; zVAD, z-VAD-FMK.

0006-2952/02/$ – see front matter
PII: S0006-2952(01)00879-6

membrane (IM), known as the permeability transition pore, is opened [13]. The loss of ionic and osmotic asymmetry across the IM may cause swelling of mitochondria and subsequent release of apoptogenic proteins, for example apoptosis-inducing factor (AIF) and cytochrome *c*, uncoupling of oxygen consumption and synthesis of ATP with generation of reactive oxygen species.

We therefore hypothesize that proapoptotic drugs and cellular proteins that belong to the apoptotic machinery may directly or indirectly affect ionic efflux/influx across the IM. A persistent proton gradient, however, is very important in generating energy under aerobic conditions: generation of proton-motive force and oxidative phosphorylation can occur only if the IM remains impermeable for the passive transport of protons. The mitochondrial uncoupler FCCP is able to dissipate the gradient of protons across the IM and therefore appears to alter mitochondrial functions in a manner similar to that of events occurring during apoptosis.

We therefore examined the possibility of inducing PCD in two haematopoetic cell lines of myeloid and lymphoid origin by incubating cells with different concentrations of FCCP *in vitro*. Furthermore, we tested the ability of FCCP to alter the time course of PCD induced by the serine/threonine protein kinase inhibitors Sts and chelerythrine (Che). These substances are potent and rapid inducers of apoptosis that interfere directly with the cellular signaling machinery and do not primarily affect the DNA. It is reasonable to assume that mitochondria play a pivotal role in this kind of PCD and that the ionic homeostasis in mitochondria, altered by FCCP, may influence the time course of apoptosis evoked by Sts and Che.

2. Materials and methods

2.1. Materials

Staurosporine (antibiotic AM-2282), chelerythrine (1, 2-dimethoxy-*N*-methyl[1,3] benzodioxolo [5,6-*c*] phenanthridinium chloride) and FCCP were purchased from Sigma; aurintricarboxylic acid and propidium iodide were from Calbiochem; 4-[3-(4-iodophenyl)-2-(4-nitrophenyl)-2*H*-5-tetrazolio]-1,3-benzene disulfonate (WST-1) and 1-methoxy-PMS (1-methoxyphenazine methosulphate) from Serva; zVAD from Bachem; NAD^+ from Roche. Stock solutions were made by dissolving drugs in DMSO or DMF; they were stored at -20°. For Western blotting mouse monoclonal antibodies C2–10 for poly-(ADP-ribose) polymerase (PARP) (Biomol), clone 19 for CPP-32 (Transduction Laboratories) and clone JLA20 for actin (Calbiochem) were used. Secondary antibodies employed were horseradish peroxidase-conjugated anti-mouse IgG from Bio-Rad and goat anti-mouse IgM from Calbiochem. Standard chemicals were purchased from Merck or Sigma.

2.2. Cells and cell culture

CCRF-CEM (acute T lymphoblastic leukemia) and HL60 cells (acute promyelocytic leukemia) were purchased from ATCC and maintained in RPMI-1640 medium supplemented with 10% (v/v) fetal calf serum, penicillin (100 unit/mL) and streptomycin (100 μg/mL) (Biochrom). Cells were cultivated in 5% CO_2/95% humidified air at 37°. Cell density during experiments was adjusted to 1.2×10^6–1.5×10^6 mL^{-1} medium by adding fresh medium on the day of the experiment. Drugs in different concentrations were added to cell culture medium from stock solutions.

2.3. Flow cytometric apoptosis assay

Assay was performed according to standard procedure with slight modifications. Briefly, 3×10^5 cells were washed once in HBSS, and 70 μL of labeling solution (10 mM HEPES, pH 7.4, 5 mM $CaCl_2$, 2.66% of FITC-conjugated Annexin V solution (Roche)) was added to the cell pellet. It was incubated for 10 min at 37° and diluted with 300 μL of solution containing 10 mM HEPES, pH 7.4, 5 mM $CaCl_2$, 0.01 mg/mL propidium iodide. Flow cytometry was performed on a FACScan (Becton Dickinson) with an excitation wavelength of 488 nm and an emission wavelength of 525 nm (FL1) for Annexin V-FITC and 620 nm (FL3) for propidium iodide. Five thousand events were analyzed. Living, apoptotic and dead cell populations were gated out and calculated.

2.4. Pulsed-field gel electrophoresis and conventional DNA gel electrophoresis

Pulsed-field gel electrophoresis (PFGE) was performed using a CHEF-DRIII pulsed-field electrophoresis system (Bio-Rad): 5×10^6 cells were washed in PBS, then resuspended in 63 μL of cell suspension buffer (10 mM Tris, pH 7.2, 20 mM NaCl, 50 mM EDTA) and equilibrated for 5 min at 50°.

Next, 37 μL of 2% pulsed-field certified agarose (Sigma) was added. The mix was incubated for 7 min at 50° and then transferred to the plug molds. The solidified blocks were incubated overnight at 55° in proteinase K reaction buffer (100 mM EDTA, pH 8.0, 0.2% Na desoxycholate, 1% Na laurylsarcosine, and 0.5 mg/mL proteinase K) and then transferred onto 1.4% agarose gels. The running time was 9 hr at 9 V/cm with a 4–8 s switch time ramp at an included angle of 120°. DNA was visualized with ethidium bromide staining. To detect small DNA fragments 100 μg/mL RNAse A (Serva) was added to the proteinase K reaction buffer. The samples were then incubated for 1 hr at 55°, extracted once with 1:1 phenol/chloroform, precipitated with ethanol and conventional DNA gel electrophoresis was performed.

2.5. Western blotting for PARP, actin and CPP-32

Trypan blue negative cells (1.5×10^6) were lysed in 60 μL of lysis buffer containing 62.5 mM Tris, pH 6.8, 6 M urea, 2% SDS, 10% glycerol, 0.00125% bromphenol blue, 5% β-mercaptoethanol, passed three times through a 25G needle and incubated for 15 min at 65°. A total of 10 μL of lysate, corresponding to approximately 10 μg of protein per lane, was subjected to SDS-PAGE analysis and subsequently transferred to nitrocellulose membrane (Sartorius). Blots were incubated overnight with mouse monoclonal antibodies C2–10 for PARP (1:200), clone 19 for CPP-32 (1:1000), clone JLA20 for actin (1:4000) and then with secondary horseradish peroxidase-conjugated goat anti-mouse IgG (Bio-Rad) or goat anti-mouse IgM antibodies (Calbiochem) (both 1:2000). For visualization of bands, detection was performed using the ECL chemiluminescence system (Amersham).

2.6. Determination of caspase-3 activity

The enzymatic activity of caspase-3 in CCRF-CEM cells was performed according to Hasegawa *et al.* [14]. Briefly, 2×10^6 cells were washed once with PBS and lysed in 150 μL of lysis buffer containing 10 mM Tris, pH 7.4, 1 mM EDTA, 10 mM EGTA, and 30 μg/mL digitonin for 15 min at 37°. Lysates were centrifuged at 12,500 *g* for 5 min and clear supernatants collected. A 70 μL of lysate was diluted with 430 μL of lysis buffer, and fluorogenic substrate DEVD-AFC was added at a sample concentration of 37.5 μM. The substrate mix was incubated for 15 min. Fluorescence at 0 and 15 min corresponding to the release of 7-amino-4-trifluoromethylcoumarin (AFC) was monitored with a spectral fluorimeter Hitachi F-2000 using an excitation wavelength of 400 nm and an emission wavelength of 505 nm. The fluorescence intensities were compared with those of the control samples, which were defined as 100%.

2.7. Assay for poly-(ADP-ribose) polymerase

The activity of PARP in CCRF-CEM cells was measured according to the method of Yoshihara *et al.* [15]. Briefly, 1.5×10^6 cells were washed once with buffer containing 10 mM Tris, pH 7.8, 1 mM EDTA, 4 mM $MgCl_2$, 10 mM DTT, 0.25 M sucrose, resuspended in 100 μL of the same buffer and kept on ice for 30 min. Of the substrate mixture 200 μL containing 50 mM Tris, pH 8.5, 37.5 mM $MgCl_2$, 0.5 mg/mL BSA, 50 μM ^{3}H-NAD^+ (0.1 MBq/mL, NEN) was added. The samples were incubated at 37° for 25 min, precipitated, washed twice with 10% TCA and suspended with 3 mL of scintillation liquid (Rotiszint, Roth). Acid insoluble radioactivity was determined using the liquid scintillation counter Beckman LS5000 TA. The PARP activity of treated cells was expressed as a percent of PARP activity of the control samples defined as 100%.

2.8. Determination of intracellular NAD^+ content

Approximately 0.5 M of Trypan blue negative cells were collected and washed once in PBS. To determine of the intracellular NAD^+ 100 μL of 0.5 M (w/v) perchloric acid was added to the cell pellet and the lysates were incubated at 4° for 15 min. Then 30 μL of neutralization buffer containing 2 N KOH, 0.2 M K_2HPO_4/KH_2PO_4, pH 7.5 was added, the lysates were centrifuged at 12,500 *g* for 3 min and clear supernatants were collected and stored at −70°.

We applied the cycling assay based on NAD(P)H-dependent electron transfer through 1-methoxy-PMS to WST-1 with its subsequent reduction to water-soluble formazan. Oxidized NAD^+ was subsequently reduced by dehydrogenases (alcohol dehydrogenase (ADH) added to the reaction mix). The reduced WST-1 can be measured spectrophotometrically at 450 nm so that the indicator reaction can be omitted. We compared this assay with a more commonly used method [16] and obtained the same sensitivity and superior accuracy of measurement. Cell extracts (10 μL) were pipetted onto a 96-well plate, to which 150 μL of reaction mix containing 60 mM Gly–Gly buffer, pH 7.4, 1.63 mM WST-1, 65.3 μM 1-methoxy-PMS, 60 mM nicotinamide, 300 mM ethanol and 20 unit ADH was added.

The plates were incubated for 40 min at 37° and absorbance was measured using an ELISA reader (Biotek instruments) at a wavelength of 450 nm. The intracellular NAD^+ content was determined using a calibration curve calculating according to external standards.

2.9. Determination of intracellular ATP content

The intracellular ATP content was determined by luciferin-luciferase assay (Labsystems) according to the manufacturer's instructions. Briefly, neutralized acid cell extracts also used for intracellular NAD^+ determination were diluted 1:50 for HL60 cells and 1:100 for CCRF-CEM cells with a solution containing 0.1 M Tris acetate, pH 7.75, 2 mM EDTA. Diluted cell extract (50 μL) was pipetted onto a white 96-well plate (Labsystems) and 110 μL of Tris acetate buffer along with 40 μL of ATP monitoring reagent were added using an automatic dispensing system, so that the ATP monitoring reagent was finally diluted 1:5. Light output was measured using the chemiluminometer Lucy-1 (Anthos) equipped with Microwin 3.1 ELISA software adapted for 96-well plate (Biotek instruments). Intracellular ATP content was calculated from the ATP standard curve and expressed in nanomol per 10^6 cells.

2.10. Statistical analysis

The Student's *t*-test was used to determinate statistical significance. The level of significance was defined as $P < 0.05$.

3. Results

3.1. Induction of apoptosis after treatment with FCCP in CCRF-CEM and HL60 cell lines

We first examined the time and concentration dependence of apoptosis induced by FCCP in CCRF-CEM and HL60 cell lines. Different concentrations of FCCP were added to HL60 and CCRF-CEM cells throughout. Furthermore, we tested whether known inhibitors of apoptosis such as an inhibitor of caspases z-VAD-FMK (zVAD) and aurintricarboxylic acid (ATA), an activator of some protein tyrosine kinases and an inhibitor of Ca, Mg-dependent endonucleases, exert a protective effect on FCCP-induced cell death. In this case, 50 μM z-VAD or 500 μM ATA were added to the cells 1 hr before starting treatment with 20 μM FCCP. For each viability curve, three independent experiments were performed, each of them in duplicate. Fig. 1A and B shows the time course of apoptosis evoked by various concentrations of FCCP, measured at five different times using the Annexin V assay.

The onset of apoptosis occurred 3 hr after starting the experiment in both cell lines. At 24 hr after commencement of treatment with 20 μM FCCP approximately 65% of HL60 cells and 90% of CCRF-CEM cells had undergone apoptosis, whereas approximately 25% of cells in both cell lines died when 4 μM FCCP was used. Pretreatment with zVAD resulted in a statistically significant delay in FCCP-induced cell death in HL60 cells exposed to FCCP: survival increased by about 35–40% within the first 12 hr,

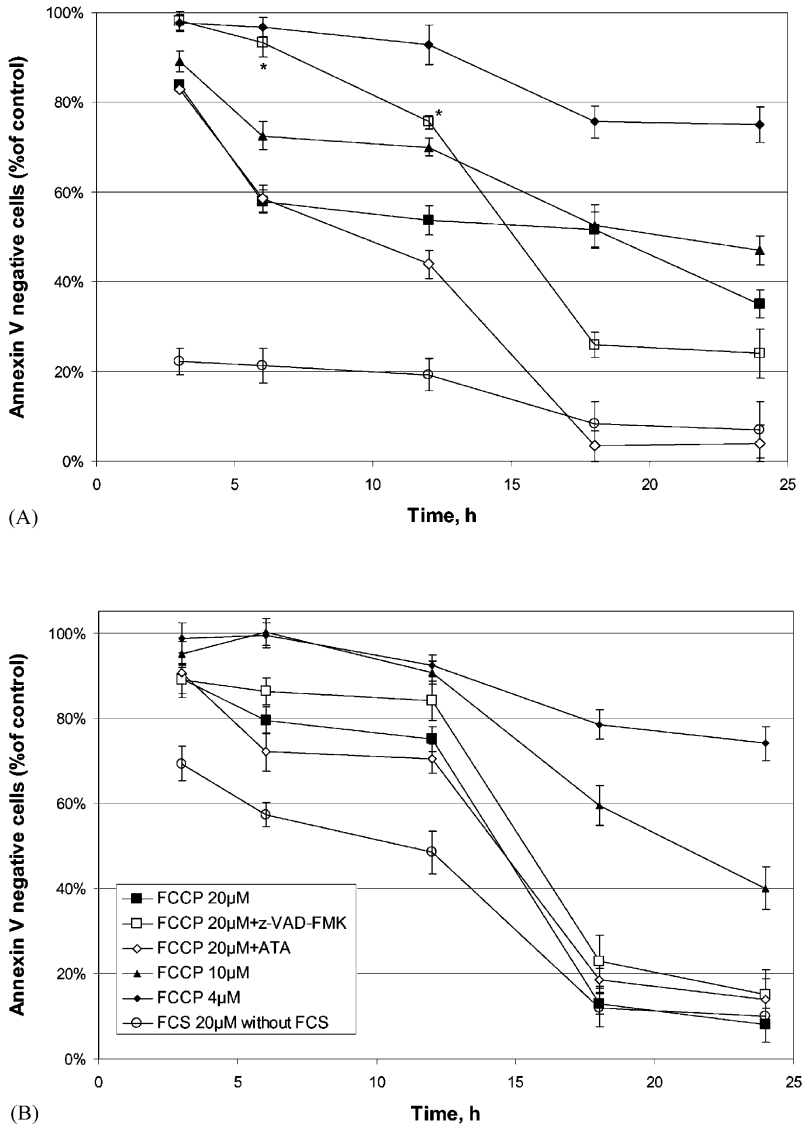

Fig. 1. Kinetics of programmed cell death induced by FCCP in HL60 (A) and CCRF-CEM (B) cells. After 3, 6, 12, 18, 24 hr aliquots of cell suspensions incubated with the drugs were collected, stained with Annexin V and analyzed by flow cytometry as described in Section 2. The relative amount of Annexin V negative cells in the whole cell population were calculated and normalized to the survival of cells in the control cell population collected at the same time point. At each time point at least 80% of the cells of the control cell population were Annexin V negative. Asterisks denote a statistically significant delay of FCCP-induced cell death caused by zVAD in HL60, but not in CCRF-CEM cells.

as compared with the viability curve for 20 μM FCCP alone ($P < 0.05$). In contrast, the protective effect of zVAD was statistically not significant in CCRF-CEM cells (Fig. 1A and B). Long-term survival of HL60 cells using 50 μM zVAD remained unaffected, and we did not observe any significant differences in cell survival after 18 hr of coincubation with FCCP.

Surprisingly, ATA slightly accelerated occurrence of apoptosis in CCRF-CEM and HL60 cells (Fig. 1A and B).

The kinetics of apoptosis induction depended on the addition of fetal calf serum (FCS) to the incubation medium: when the maintenance medium supplemented with 10% FCS was removed before starting FCCP treatment and replaced with the same growth medium without FCS, cell death occurred faster in both HL60 and CCRF-CEM cells (Fig. 1A and B). Light microscopically the cells showed typical morphological features of apoptosis such as nucleus condensation, abnormal light scattering, and membrane blebbing.

FCCP-induced apoptosis took place without appearance of typical oligonucleosomal DNA fragmentation detectable by conventional DNA agarose gel electrophoresis (data not shown) despite pronounced degradation of DNA. Pulsed-field gel electrophoresis revealed 10–50 kbp DNA fragments after treatment of cells with FCCP in both cell lines. Degradation of genomic DNA was particularly distinctive in HL60 cells (Fig. 2A). Western blot analysis showed apoptotic PARP cleavage patterns and CPP-32 decrease following FCCP treatment (Fig. 2B).

3.2. Induction of apoptosis by chelerythrine and staurosporine in CCRF-CEM and HL60 cells

We used inhibitors of serine threonine protein kinases Che and Sts to investigate the ability of FCCP to modulate the time course of PCD induced by these drugs. Both substances are rapid and potent inducers of apoptosis in haematopoietic cell lines and do not primarily damage DNA.

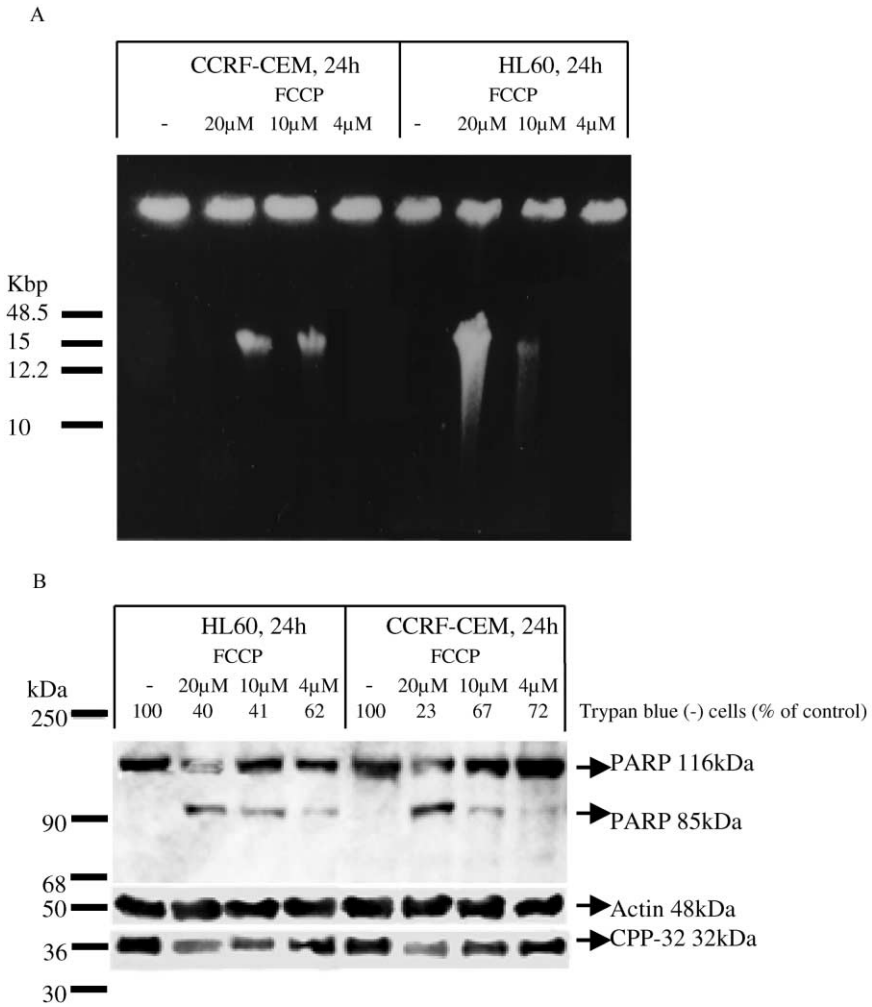

Fig. 2. Apoptotic changes in HL60 and CCRF-CEM cells exposed to various concentrations of FCCP: DNA fragmentation into large (10–50 kbp) fragments shown by PFGE (A) and PARP-cleavage and CPP-32 decrease in FCCP-treated HL60 and CCRF-CEM cells assessed by Western blotting (B). The viability of cells was estimated by Trypan blue staining and expressed as a percent of control, defined as 100%. To detect PARP cleavage, FCCP-treated cell lysates were run on 8% SDS-PAGE gel. A 15% SDS-PAGE gel was used to assess the decrease or disappearance of CPP-32 (procaspase-3). Actin was detected on 15% SDS-PAGE gel to assure that an equivalent amount of protein from each sample was loaded in each lane.

The number of living, apoptotic and dead cells was determined using the Annexin V assay and expressed as a mean percentage of total cell number (100%). Three independent experiments were performed, each in duplicates. After 6 hr addition of Sts (300 nM) or Che (10 μM) to HL60 and CCRF-CEM cells approximately 70–90% apoptotic cell death was observed using the Annexin V assay and Trypan blue staining. The onset of apoptosis occurred within 30 min after Che treatment and within 120 min after Sts treatment (Fig. 3A–C).

DNA-agarose gel electrophoresis of small DNA fragments revealed typical oligonucleosomal DNA laddering within 3 hr after exposure to Che and 6 hr after exposure to Sts (Fig. 4A).

Western blot analysis of cell lysates treated with Sts and Che showed a typical PARP cleavage pattern (Fig. 5A–C). Remarkably, PARP cleavage and decrease in intracellular CPP-32 (pro-caspase-3) were more pronounced when lower concentrations of Che (10 μM) were used, as compared to its higher concentrations (20 μM), although cell

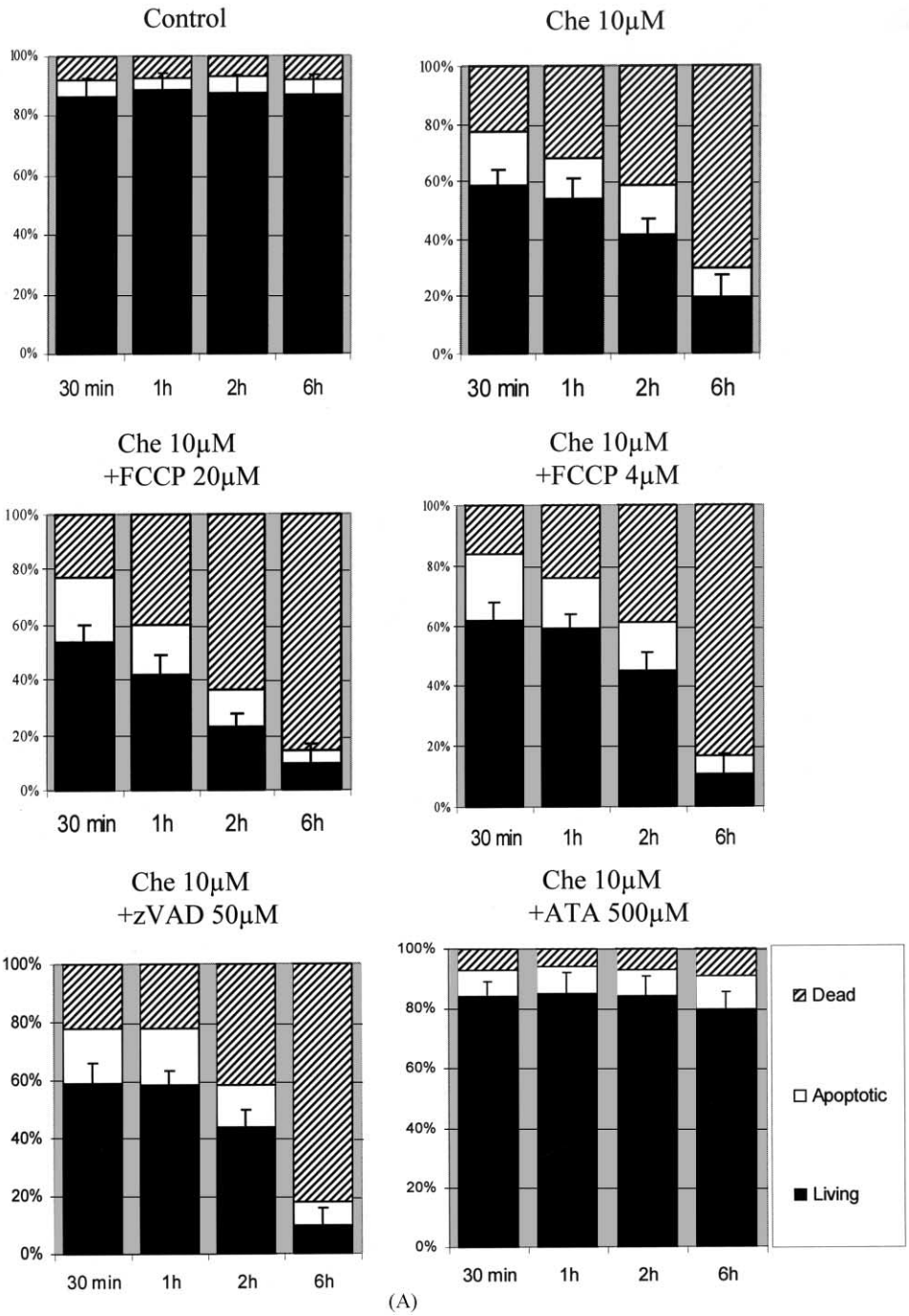

Fig. 3. Viability of HL60 (A) and CCRF-CEM (B) cells measured at four different times after starting incubation with 10 μM Che or at five different times after exposure to 300 nM Sts in CCRF-CEM cells (C). When indicated, FCCP, ZVAD or ATA was added 1 hr before starting treatment with either Che or Sts.

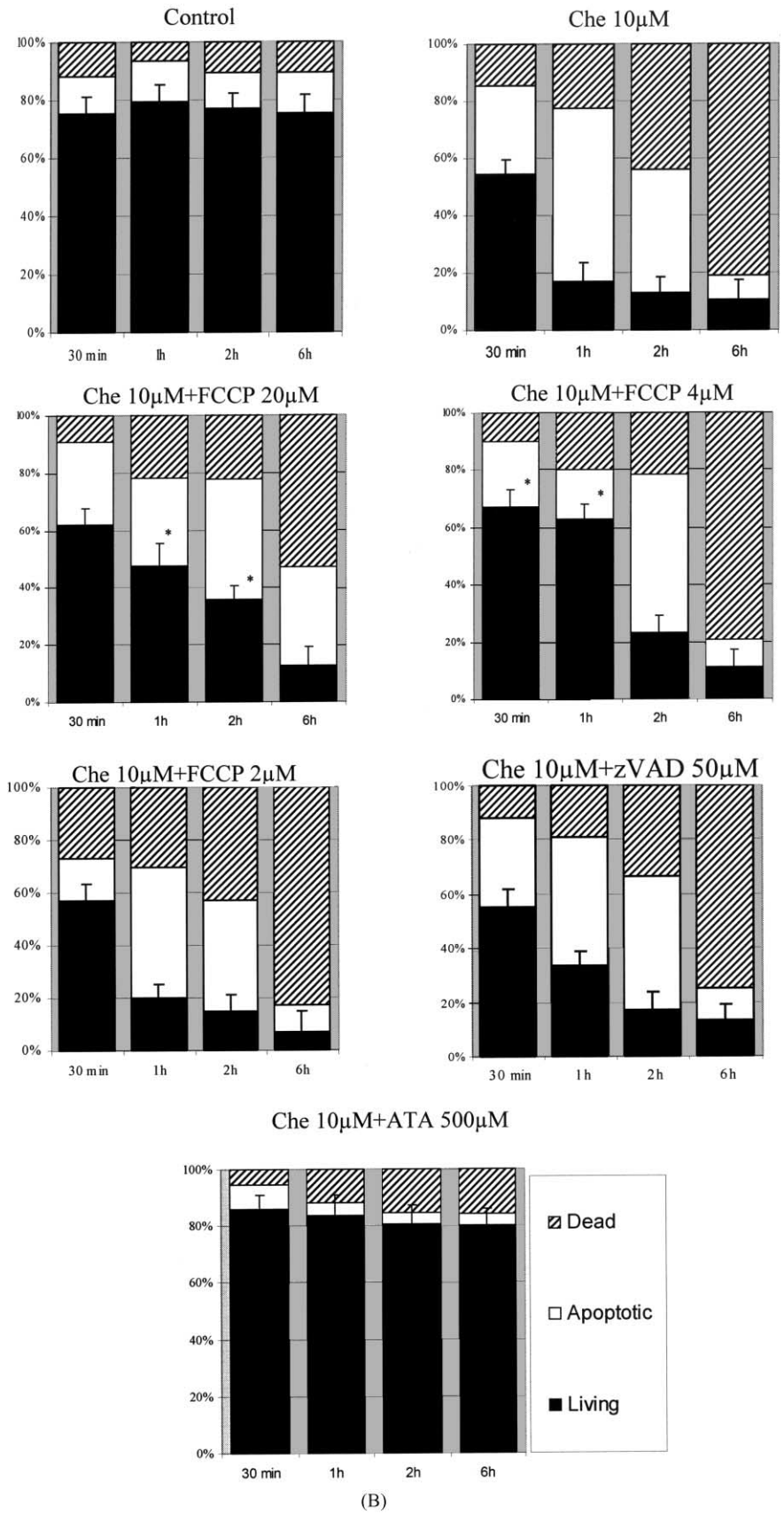

(B)

Fig. 3. (*continued*).

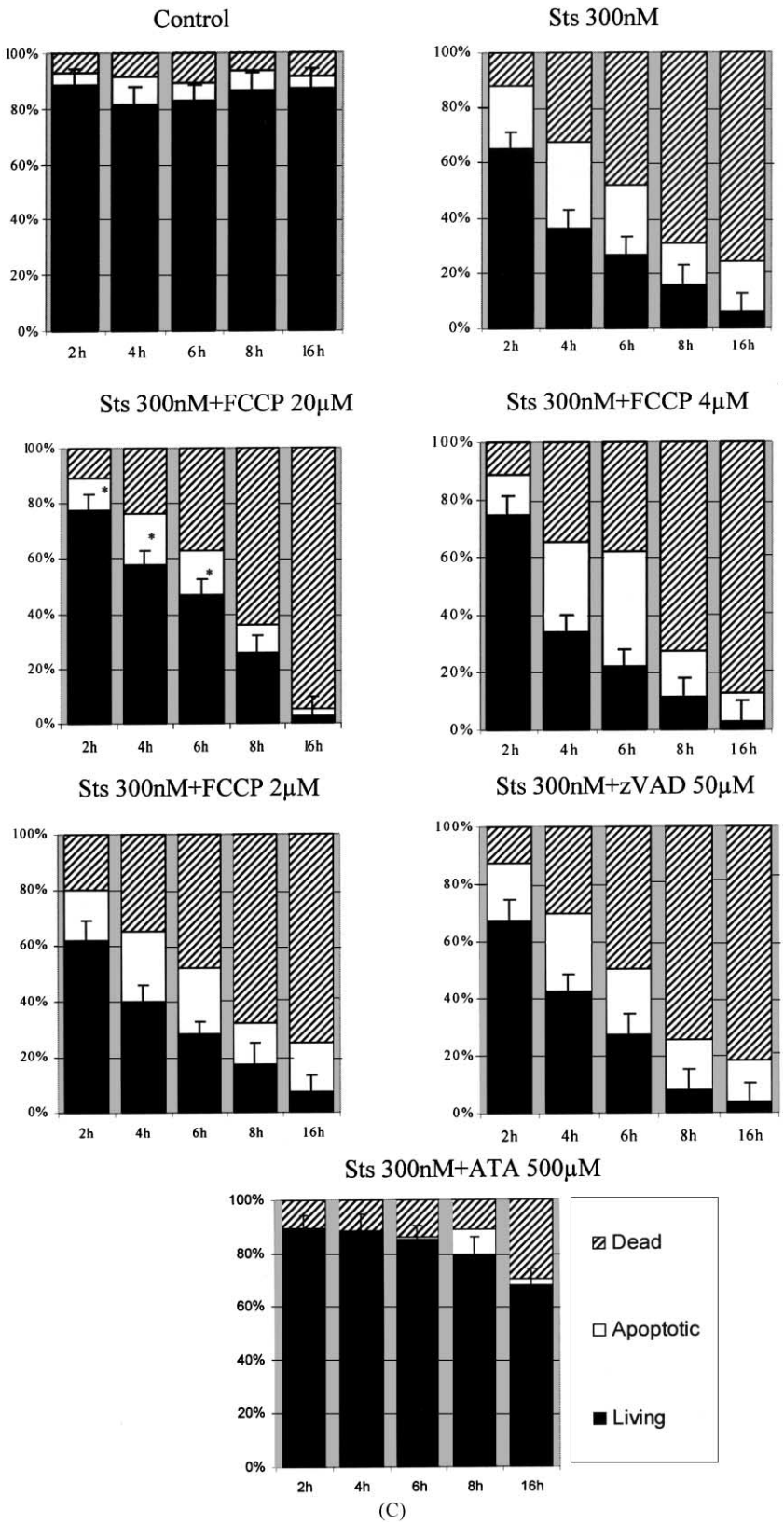

(C)

Fig. 3. (*continued*).

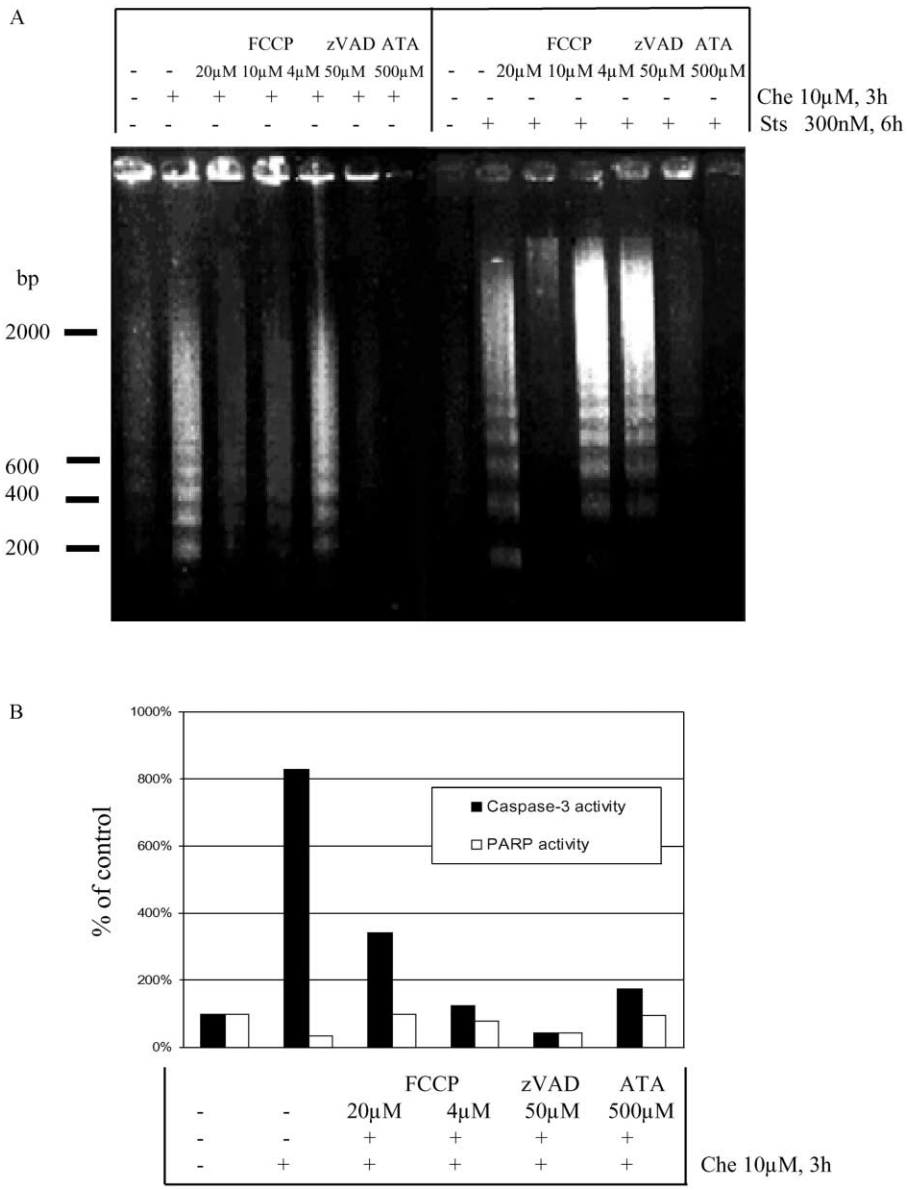

Fig. 4. Formation of small DNA fragments in CCRF-CEM cells at either 3 hr of incubation with Che (lanes 1–7) or 6 hr of treatment with Sts (lanes 8–14) with or without addition of modulators (A) shown by conventional DNA agarose gel electrophoresis. Alterations in caspase-3 and PARP activity after 3 hr of incubation with Che in CCRF-CEM cells (B). Both PARP and caspase-3 activity were calculated as a percentage of PARP and caspase-3 activity in the control samples, defined as 100%. The data presented are from one of three independent experiments with the same results.

death shown by Trypan blue staining occurred in a dose-dependent manner (Fig. 6).

Levels of caspase-3 activity increased about 8-fold after Che treatment. In contrast, PARP activity decreased by more than 50%, as compared to the control (Fig. 4B).

3.3. Protection against Che- and Sts-induced apoptosis by FCCP in CCRF-CEM but not in HL60 cells: comparison with other known inhibitors of apoptosis such as zVAD and ATA

Addition of the mitochondrial uncoupler FCCP caused a remarkable delay in onset of apoptosis, whether induced in CCRF-CEM cells by either Sts or Che. The protective effect of FCCP was confirmed by Trypan blue staining. FCCP at a concentration of 2 μM or less did not exhibit any protective impact on this kind of apoptosis. The optimal inhibitory effect of FCCP was achieved at a concentration of 20 μM for Sts-induced and 4 μM for Che-induced apoptosis: about 50% more cells survived after coincubation with FCCP, as compared to treatment with Che alone, and 25% more cells were alive after 6 hr of treatment, as compared to exposure to Sts alone. Advantage in survival of CCRF-CEM cells, preincubated with FCCP, was statistically significant at time points 30 min, 1 and 2 hr for Che-induced apoptosis and at time points 2, 4 and 6 hr for Sts-induced apoptosis, as compared to cells treated with Che or Sts alone ($P < 0.05$). Measurements of cellular

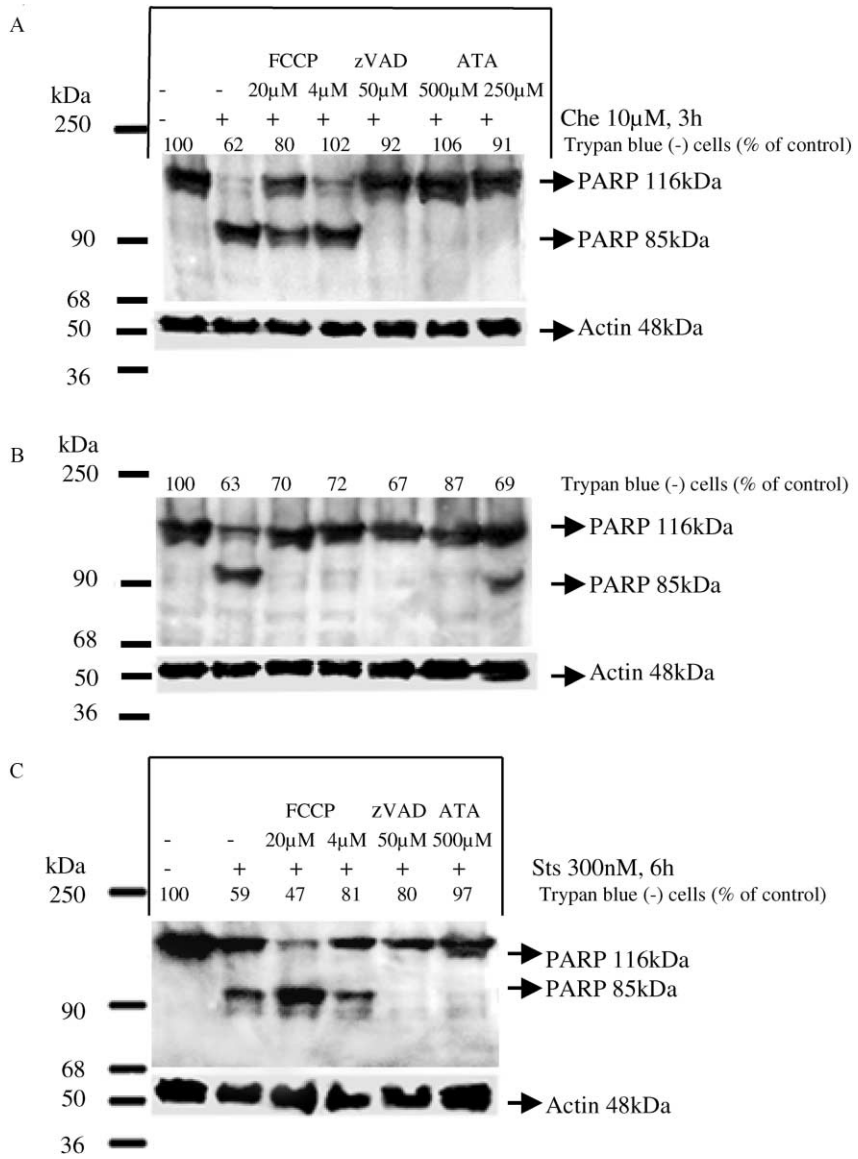

Fig. 5. Prevention of PARP cleavage induced by incubation of HL60 (A) and CCRF-CEM (B) with Che for 3 hr or by treatment of CCRF-CEM cells with Sts for 6 hr (C) using modulators.

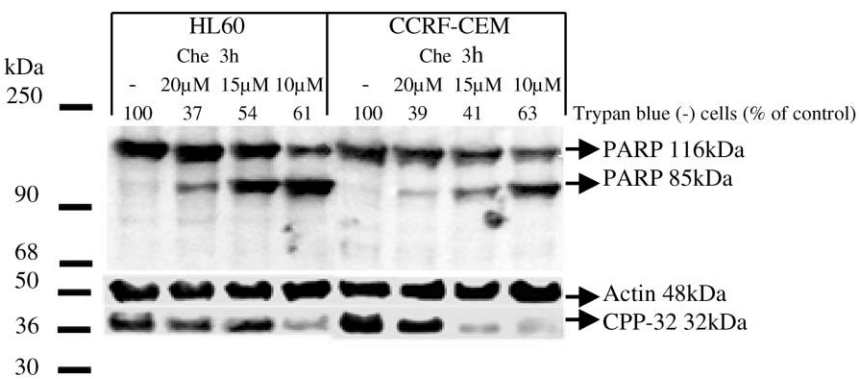

Fig. 6. Cleavage of PARP in and decrease in the intracellular CPP-32 content of HL60 and CCRF-CEM cells after treatment with different concentrations of Che for 3 hr.

viability after exposure to Che or Sts in CCRF-CEM cells, performed at later time points, did not reveal any advantage of pre-treatment with FCCP on long-term survival (Fig. 3B and C).

Coincubation of CCRF-CEM cells with FCCP also diminished DNA fragmentation to small (180 bp) fragments as compared with cell samples treated with either Sts or Che alone (Fig. 4A). FCCP had no influence on the degree of PARP cleavage by Sts-induced apoptosis, but delayed the appearance of 85 kDa PARP-cleaved fragments during Che-induced apoptosis in CCRF-CEM cells (Fig. 5B and C). In HL60 cells FCCP failed to alter the time course of apoptosis induced by Che (Fig. 3A), but slightly delayed the proteolytic cleavage of PARP after exposure to Che (Fig. 5A).

The activity of caspase-3 in CCRF-CEM cells after preincubation with FCCP was about 2.5-fold decreased as compared to incubation with serine/threonine protein kinase inhibitors alone, but was not completely abolished. In addition, pretreatment with FCCP restored a decrease in PARP activity evoked by Che (Fig. 4B).

We also investigated the protective effect of zVAD. The caspases inhibitor zVAD at a concentration of 50 μM was able to prevent DNA fragmentation in CCRF-CEM cells, treated with either Sts or Che. Proteolytic degradation of the caspase-3 substrate PARP was also delayed (Fig. 5A–C). The inhibitory effect of zVAD lasted only 2 hr for Che-induced apoptosis and 4 hr for Sts-induced apoptosis: cell survival increased by about 20% in both cases, this difference not being statistically significant compared to the treatment with Che or Sts alone, as shown by the Annexin V assay (Fig. 3A–C).

ATA at a non-toxic concentration of 500 μM completely inhibited apoptosis induced by Che and Sts. PARP cleavage, CPP-32 precursor decrease, and the formation of oligonucleosomal DNA fragments were also totally abolished. Cellular morphology remained unaltered. Lower concentrations of ATA (250 μM) prevented Che-induced apoptotic cell death in HL60 cells, whereas in CCRF-CEM cells they failed to protect the cells from deleterious effects of Che (Fig. 5A and B).

3.4. Depletion of the intracellular NAD^+, NADH, NADPH and ATP levels after exposure of HL60 and CCRF-CEM cells to Che

Three hours after starting treatment with 10 μM Che a strong decrease was detected in the intracellular NAD^+ and ATP content in both cell lines. Two independent experiments conducted in triplicate were performed. ATP depletion was more pronounced in HL60 cells, whereas in CCRF-CEM cells almost complete NAD^+ depletion occurred. Only ATA, but not FCCP or zVAD, was able to return the intracellular NAD^+ and ATP levels in both cell lines to close to control values although some protective effect of FCCP and zVAD on intracellular ATP levels in CCRF-CEM cells and on NAD^+ levels in HL60 cells was observed (Fig. 7A and B).

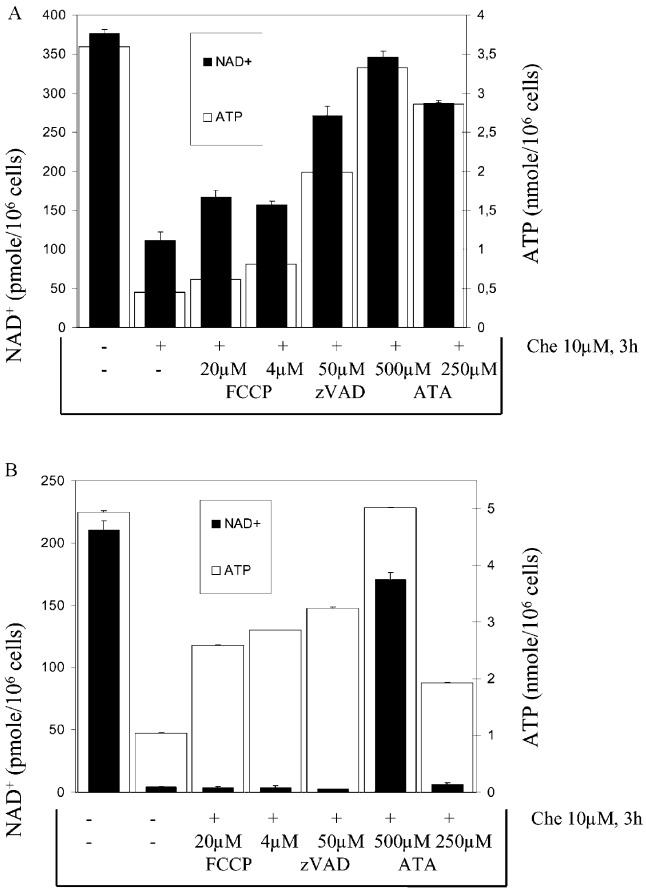

Fig. 7. Decrease in intracellular NAD^+ and ATP content in HL60 (A) and CCRF-CEM cells (B) after 3 hr of treatment with 10 μM Che. Intracellular NAD^+ content was calculated using external standards measured simultaneously.

4. Discussion

Alterations in cellular mitochondrial function appear to play a key role in the development of apoptosis induced by several agents such as dexamethasone [17], TNF-α [18], Fas and nerve growth factor (NGF) withdrawal [19]. Some authors [1,7] have reported that cells undergoing apoptosis show an early reduction in the incorporation of mitochondrial membrane potential (ψ_m)-sensitive dyes such as rhodamine 123 and JC-1, indicating a drop in ψ_m. Functional experiments indicate that the preapoptotic dissipation of mitochondrial membrane potential occurs as a result of a sudden increase in the permeability of the inner mitochondrial membrane to low molecular weight solutes.

The mitochondrial permeability transition pore can also be opened by protonophoric uncouplers such as FCCP [20,21]. Our interest focused on the ability of FCCP to mimic the mitochondrial events thought to occur during apoptosis. If mitochondrial permeability transition is a

central coordinating event of the apoptotic effector phase, FCCP as a potent mitochondrial uncoupler should induce apoptosis itself and show a synergistic effect with other non-DNA-damaging apoptosis-inducing agents like Sts and Che. In the present study we showed that FCCP was able to induce apoptosis in cells of lymphoid (CCRF-CEM) and myeloid (HL60) origin, while other investigators also induced apoptosis by FCCP in cells of neuronal origin [26].

To us, the effect of FCCP appears weak as compared to apoptosis induced by etoposide [34] or kinase inhibitors. The kinetics of apoptotic change was relatively slow. FCCP failed to induce oligonucleosomal DNA fragmentation, and only large DNA fragments (approximately 15–50 kb) were detectable.

The reason why apoptosis was more pronounced and occurred much faster in serum-free medium is unclear. We assume that withdrawal of survival factors present in FCS may inactivate some antiapoptotic pathways that interfere with proapoptotic mechanisms triggered by exposure of cells to FCCP. Alternatively, FCCP may be partially inactivated by binding to serum proteins.

Sts- and Che-induced apoptoses have been useful models for studying some of the features of the basic mechanics of PCD [22–24]. Apoptosis occurred very rapidly (90% cell death within 6 hr after incubation with these compounds), and a 4- to 10-fold increase in caspase-3 activity with cleavage of its typical substrates such as PARP, CPP-32 and oligonucleosomal DNA fragmentation was observed.

This study also demonstrates that FCCP did not accelerate the onset of apoptosis, but rather protected the lymphoid CCRF-CEM cells from Che- and Sts-induced apoptosis. A protective effect of FCCP on the TNF-α-induced apoptosis was also described by [18].

The protective concentration of FCCP is generally, at least for Che-induced apoptosis, somewhat lower than is the concentration required for the induction of apoptosis itself. Pretreatment with FCCP caused a diminished formation of oligonucleosomal DNA fragments and partially prevented an increase in caspase-3 activity. In promyelocytic HL60 cells FCCP failed to increase the survival fraction after treatment with either Che or Sts although we observed the delayed proteolytic cleavage of PARP in both cell lines (Fig. 5A and B). We observed, however, that CCRF-CEM cells are much more sensitive to the apoptosis-inducing effect of serine/threonine protein kinase inhibitors as compared to HL60 cells, whereas the sensitivity of these cell lines to FCCP is exactly the opposite. Obviously, in HL60 cells cytotoxic effects of FCCP prevail over its antiapoptotic features.

The mechanism of FCCP-induced prevention of apoptosis remains unclear although it is evident that FCCP interferes with basic components of the apoptotic machinery, e.g. prevents the proteolytic cleavage of caspase-3 substrates, oligonucleosomal DNA fragmentation and the appearance of phosphatidylserine on the outer cell membrane surface. In addition, this study shows that FCCP did not upregulate Bcl-2 (data not shown). Some investigators have reported that impaired mitochondrial function and FCCP itself can activate some signaling factors, such as NF-κB and different kinases [27,28]. However, the general mechanism permitting mitochondria to prevent induction of apoptosis remains unclear.

Previous work by other investigators [25,33,34] has suggested that the decrease in mitochondrial membrane potential measured using potential-sensitive fluorescent stains, such as JC-1 and rhodamine 123, did not take place in all cell lines when using concentrations of FCCP from 1 to 50 μM.

The caspases inhibitor zVAD showed, in our hands, only a weak apoptosis-inhibitory effect, and when using a specific caspase-3 inhibitor, z-DEVD-FMK, the effect was similar. Some authors [29] described an inhibitory effect of zVAD on Sts-induced apoptosis in SV40-transformed human fibroblasts (GM701 cell line), SKW 6.4 and CHO cells. Weil *et al.* [30], however, demonstrated that z-VAD was effective against Sts-induced apoptosis in E13 mouse embryo cell line but not in four cell mouse embryos.

We have observed some peculiarities that are typical for Che-induced apoptosis, at least in two investigated haematopoetic cell lines: first, Che-induced apoptosis was accompanied by strong depletion of intracellular NAD^+ and ATP pools, which occurred already 3 hr after commencement of Che treatment (Fig. 7A and B), and second, the Che concentrations applied correlated directly with cell death assessed by Trypan blue staining and inversely with the grade of PARP cleavage, shown by Western blotting (Fig. 6). Thus, in addition to activation of caspase-3 and subsequent execution of the apoptotic program, Che causes depletion of energy equivalents in both cell lines, which may result in necrosis, particularly at higher concentrations. The rapidly occurring energy depletion may therefore explain why the antiapoptotic effects of zVAD and FCCP did not prolong cell survival.

It is well known that alkylating substances such as 1-methyl-3-nitro-1-nitroso-guanidine (MNNG), temozolomide [35], hydrogen peroxide [36] and ricin [37] induce delayed cell death by causing PARP activation and subsequent wasteful consumption of NAD^+. However, NAD^+ depletion found after treatment with Che is not due to enhanced PARP activity. First, we did not observe the activation of PARP after treatment of CCRF-CEM cells with Che (Fig. 4B), and second, preincubation of HL60 and CCRF-CEM cells with the PARP inhibitor 3-aminobenzamide before treatment with Che did not result in long-term cellular protection (data not shown).

It has been reported [31] that ATA, another inhibitor of Che- and Sts-induced apoptosis can stimulate tyrosine phosphorylation. The protection of cells from apoptosis by ATA, induced by the serine/threonine protein kinase inhibitors Sts and Che, may therefore be explained by the

triggering of antiapoptotic kinase pathways. Involvement of kinases appears to be an ancillary event in the time course of apoptosis, induced by mitochondrial uncouplers, and therefore ATA does not protect cells against FCCP-induced apoptosis.

References

[1] Petit PX, Susin S-A, Zamzami N, Mignotte B, Kroemer G. Mitochondria and programmed cell death: back to the future. FEBS Lett 1996;396:7–13.

[2] Vander Heiden MG, Chandel NS, Williamson EK, Schumacker PT, Thompson CB. Bcl-xl regulates the membrane potential and volume homeostasis of mitochondria. Cell 1997;91:625–37.

[3] Kane DJ, Sarafian TA, Anton R, Hahn H, Gralla EB, Valentine JS, Ord T, Bredesen DE, Bcl-2 inhibition of neural death: decreased generation of reactive oxygen species. Science 1993;262:1274–7.

[4] McDonald G, Shi L, Velde CV, Lieberman J, Greenberg AH. Mitochondria-dependent and -independent regulation of Granzyme B-induced apoptosis. J Exp Med 1999;189:131–43.

[5] Bredesen DE. Neural apoptosis. Ann Neurol 1995;38:839–51.

[6] Kluck RM, Martin SJ, Hoffman BM, Zhou JS, Green DR, Newmeyer DD. Cytochrome *c* activation of CPP 32-like proteolysis plays a critical role in a Xenopus cell-free apoptosis system. EMBO J 1997;16:4639–49.

[7] Susin SA, Zamzami N, Castedo M, Hirsch T, Marchetti P, Macho A, Daugas E, Geuskens M, Kroemer G. Bcl-2 inhibits the mitochondrial release of an apoptogenic protease. J Exp Med 1996;184:1331–41.

[8] Jacobson MD, Burne JF, Miyashita T, Reed JC, Raff MC. Bcl-2 blocks apoptosis in cells lacking mitochondrial DNA. Nature 1993;361:365–9.

[9] Hockenbery DM, Oltvai ZN, Yin XM, Milliman CL, Korsmeyer SJ. Bcl-2 functions in an antioxidant pathway to prevent apoptosis. Cell 1993;75:241–51.

[10] Oltvai ZN, Milliman C, Korsmeyer SJ. Bcl-2 heterodimerizes *in vivo* with a conserved homolog, Bax, that accelerates programmed cell death. Cell 1993;74:609–19.

[11] Schendel SL, Xie Z, Montal MO, Matsuyama S, Montal M, Reed JC. Channel formation by antiapoptotic protein Bcl-2. Proc Natl Acad Sci USA 1997;94:5113–8.

[12] Green DR, Reed JC. Mitochondria and apoptosis. Science 1998;281:1309–12.

[13] Quian T, Herman B, Lemasters J. Mitochondrial permeability transition in pH-dependent reperfusion injury to rat hepatocytes. Am J Physiol 1997;273:C1783–92.

[14] Hasegawa J, Kamada S, Kamiike W, Shimizu S, Imazu T, Matsuda H, Tsujimoto Y. Involvement of CPP-32/Yama(-like) proteases in Fas-mediated apoptosis. Cancer Res 1996;56:1713–8.

[15] Yoshihara K, Itaya A, Hironaka T, Sakuramoto S, Tanaka Y, Tsuyuki M, Inada Y, Kamiya T, Ohnishi K, Honma M, Kataoka E, Mizusawa H, Uchida M, Uchida K, Miwa M. Poly (ADP-ribose) polymerase defective mutant cell clone of mouse L1210 cells. Exp Cell Res 1992;200:126–34.

[16] Bernofsky C, Swan M. An improved cycling assay for nicotinamide adenine dinucleotide. Anal Biochem 1973;259:452–73.

[17] Petit PX, Lecoeur H, Zorn E, Dauguet C, Mignotte B, Gougeon M-L. Alterations in mitochondrial structure and function are early events of dexamethasone-induced thymocyte apoptosis. J Cell Biol 1995; 130:157–67.

[18] Schulze-Osthoff K, Ferrari D, Los M, Wesselborg S, Peter ME. Apoptosis signaling by death receptor. Eur J Biochem 1998;254:439–59.

[19] Deckwerth TL, Easton RM, Knudson CM, Korsmeyer SJ, Johnson EM. Placement of the Bcl-2 family member Bax in the death pathway of sympathetic neurons activated by trophic factor deprivation. Exp Neurol 1998;152:150–62.

[20] Susin SA, Zamzami N, Kroemer G. Mitochondria as regulators of apoptosis: doubt no more. Biochim Biophys Acta 1998;1366:151–65.

[21] Scorrano L, Petronilli V, Bernardi P. On the voltage dependence of the mitochondrial permeability transition pore: a critical appraisal. J Biol Chem 1997;272:12295–9.

[22] Anthony ML, Zhao M, Brindle KM. Inhibition of phosphatidylcholine biosynthesis following induction of apoptosis in HL60 cells. J Biol Chem 1999;274:19686–92.

[23] Lan L, Wong NS. Phosphatidylinositol 3-kinase and proteinkinase C are required for the inhibition of caspase activity by epidermal growth factor. FEBS Lett 1999;444:90–6.

[24] Godard T, Deslandes E, Lebailly P, Vigreux C, Poulain L, Sichel F, Poul JM, Gauduchon P. Comet assay and DNA flow cytometry analysis of staurosporine-induced apoptosis. Cytometry 1999;36:117–22.

[25] Krohn AJ, Wahlbrink T, Prehn JH. Mitochondrial depolarisation is not required for neuronal apoptosis. J Neurosci 1999;19:7394–404.

[26] Dispersyn G, Nuydens R, Connors R, Borgers M, Geerts H. Bcl-2 protects against FCCP-induced apoptosis and mitochondrial membrane potential depolarisation in PC12 cells. Biochim Biophys Acta 1999;1428:357–71.

[27] Josse C, Legrand-Poels S, Piret B, Sluse F, Piette J. Impairment of mitochondrial electron chain transport prevents NF-κB activation by hydrogen peroxide. Free Radic Biol Med 1998;25:104–12.

[28] Luo Y, Bond JD, Ingram VM. Compromised mitochondrial function leads to increased cytosolic calcium and to activation of MAP kinases. Proc Natl Acad Sci USA 1997;94:9705–10.

[29] Jacobson MD, Weil M, Raff MC. Role of Ced-3/ICE family proteases in staurosporine-induced programmed cell death. J Cell Biol 1996;133:1041–51.

[30] Weil M, Jacobson MD, Raff MC. Are caspases involved in the death of cells with transcriptionally inactive nucleus? Sperm and chicken erythrocytes. J Cell Sci 1998;111:2707–15.

[31] Okada N, Koizumi S. A neuroprotective compound, aurin tricarboxylic acid, stimulates the tyrosine phosphorylation cascade in PC12 cells. J Biochem 1995;70:16464–9.

[32] Wang H-G, Rapp UR, Reed JC. Bcl-2 targets the protein kinase Raf-1 to mitochondria. Cell 1996;87:629–38.

[33] Hasmann M, Valet GK, Tapiero H, Trevorrow K, Lampidis T. Membrane potential differences between adriamycin-sensitive and -resistant cells as measured by flow cytometry. Biochem Pharmacol 1989;38:305–12.

[34] Pogrebniak A, Stoetzer OJ, Wilmanns W, Nüssler V. Alterations in mitochondrial membrane potential under influence of apoptosis-inducing substances. In: Klein HG, Seidel D, editors. Research festival, 1996. p. 39–40.

[35] Boulton S, Kyle S, Durkacz BW. Low nicotinamide mononucleotide adenilyltransferase activity in a tiazofurin-resistant cell line: effects on NAD^+ metabolism and DNA repair. Br J Cancer 1997;76:845–51.

[36] Coppola S, Nosseri C, Maresca V, Ghibelli L. Different basal NAD^+ levels determine opposite effects of poly-(ADP-ribose) polymerase inhibitors on H_2O_2-induced apoptosis. Exp Cell Res 1995;221:462–9.

[37] Komatsu N, Masami Nakagawa M, Tatsuya Oda T, Muramatsu T. Depletion of intracellular NAD^+ and ATP levels during ricin-induced apoptosis through the specific ribosomal inactivation results in the cytolysis of U937 cells. J Biochem 2000;128:463–70.